

High Temperature Stable Dysprosium modified Nano TiO₂ Photocatalyst

B. Naufal, P. Periyat*

Department of Chemistry, University of Calicut, Kerala, India - 673635.

*Corresponding author: E-Mail: pperiyat@uoc.ac.in

ABSTRACT

TiO₂ and Dy³⁺ doped TiO₂ nanocrystalline has been successfully synthesized by a modified sol-gel method. As synthesised samples of TiO₂ and Dy³⁺ doped TiO₂ were calcined at 300, 500 and 700 °C and their photocatalytic activity was compared. Characterization of the samples was carried out by various techniques such as XRD, UV/Vis Reflectance spectroscopy, FTIR and TEM. The photocatalytic activity of TiO₂ and Dy³⁺ doped TiO₂ were investigated by the degradation of methylene blue solution under UV light irradiation. The results showed that the Dy³⁺ doped TiO₂ sample calcined at 700 °C shows the highest photocatalytic activity.

KEY WORDS: Sol-gel method, photocatalyst, advanced oxidation process.

1. INTRODUCTION

Dye waste coming from textiles and food industry are one of the largest group of pollutants found in the drinking water and its colour is easily recognizable in water stream. They are either toxic or become toxic when being gradually decomposed in the ecosystem and undergo bio magnification in living organisms due to its low rate of natural degradation and also cause severe health problems. Hence many physical, chemical and biological treatment technologies are currently being employed to remove dyes waste or degrade them into non-toxic ones. However most of the organic dye waste cannot be removed using these technologies. Advanced Oxidation Processes (AOPs) is a prominent technique to remove organic dye in which the organic compounds are completely degrading into ultimate products as CO₂ and H₂O.

Among all the AOPs, photo catalytic oxidation (PCO) is the most promising one. **Error! Bookmark not defined. Error! Bookmark not defined. Error! Bookmark not defined.** Photocatalytic oxidation is a process where degradation of organic dyes and/or compounds occur by the illumination of photocatalyst without introducing any other chemicals. TiO₂, ZnO, CeO₂ and ZrO₂ are the commonly used photocatalysts. Among these TiO₂ is the promising photocatalyst because of its unique optical and physical properties and also due to its easy availability, in-expensiveness and non-toxicity. TiO₂ crystallizes mainly in to three – anatase, rutile and brookite. Majority of research work has been carried out with either anatase or rutile. Many physical, chemical and biological treatment technologies are currently being employed to remove dyes using anatase and/or rutile phase. However among these three different forms of TiO₂, anatase, rutile and brookite, generally anatase has the highest photocatalytic activity than the other two. It can be due to the high indirect band gap (E_g=3.2 eV) of anatase that enables the excited electrons to stabilize at lower level in the conduction band leading to high mobility and longer life of the excited electrons. The photocatalytic activity of semiconducting nanoparticles (TiO₂ and ZnO) is improved by doping with various rare earth dopant source.

In this work a simple modified sol-gel method was used to synthesize TiO₂ and Dy³⁺ doped TiO₂ calcined at different temperature and characterized with XRD, FTIR, DRS and TEM. Photo catalytic activities of these samples were studied by photo degradation of methylene blue under UV light. The effect of calcination temperatures on the photo catalytic activity was also been discussed.

2. EXPERIMENTAL

TiO₂ and Dy³⁺ doped TiO₂ catalysts were prepared with the raw materials of analytical grade. The raw materials used are titanium isopropoxide (Ti(OPr)₄, Aldrich, 97%), Dy(NO₃)₃ Aldrich, glacial acetic acid (Aldrich, 99.8%) and deionized water. In a typical experiment to synthesize nano TiO₂, Ti(OPr)₄ was mixed with glacial acetic acid followed by the addition of de-ionized water in small quantity with constant stirring. The Ti(OPr)₄ : acetic acid : water ratio was kept as 1:10:100. The homogenous solution was stirred for 3 hrs. It was dried at 100° C on water bath for 12 hrs. The dried powder was calcined at 300, 500 and 700° C at a heating rate of 5° C per minute and held at this temperature for 2 hrs. For the Dy³⁺ doped TiO₂ synthesis, along with the above reacting mixture calculated amount of Dysprosium (III) nitrate for 5 weight percentage were added and the same procedure is followed.

X-ray diffraction (XRD) patterns of the calcined gels were obtained with a Miniflex 600 X-ray diffractometer with CuK α radiation, $\lambda=1.54 \text{ \AA}$, Voltage 40 KV and current 15mA in the diffraction angle range 2 θ

= 10–70°. The FT IR spectra of the gel dried at 100 °C was measured by using a Jasco-FT/IR-4100 spectrometer in the wave number range 4000-400 cm⁻¹ using 70 scans for each sample. The diffuse reflectance spectra (DRS) of the catalysts in the wavelength range of 200-800 nm were obtained using a UV-Vis reflectance spectrophotometer using a Jasco-V-550 UV/VIS spectrophotometer. Morphology of the samples was examined using Transmission Electron Microscope using Hitachi SU-66000.

2.1. Photocatalytic activity evaluation: In a typical experiment 0.1 g of sample was dispersed in 50 ml of methylene blue solution having concentration of 1 x 10⁻⁴ M. This solution was stirred for 10 minutes in dark for the chemisorptions on the surface of the catalyst to avoid any absorption error. The methylene blue solution containing catalyst was then irradiated under UV photo reactor (LZC-4x Luzchem Photo reactor) with continuous and uniform stirring. The degradation of methylene blue dye was monitored by taking 5 ml aliquots at different intervals of time. These aliquots were centrifuged at 4500 rpm for 15 minute and absorption spectra of the samples were recorded using UV/Visible spectrophotometer. Methylene blue concentration was used to determine at a wavelength range of 650 – 660nm. The absorbance set at 650 – 660nm is due to the color of the dye solution and it is used to monitor the degradation of dye. The rate of degradation was assumed to obey first order kinetics and hence the rate constant for degradation k was obtained from the first order plot using equation 1.

$$\ln(A_0/A) = kt \quad (1)$$

Where A₀ is initial absorbance, A is absorbance after a time and k is the first order rate constant.

3. RESULTS AND DISCUSSION

The nano TiO₂ were synthesized by the hydrolysis of titanium tetra isopropoxide (Ti(OPr)₄) with water. Acetic acid was used as a stabilizing and catalyzing agent. Dysprosium (III) nitrate was used as a dopant source of Dy³⁺ ion.

3.1. X-ray Diffraction (XRD): XRD patterns of TiO₂ and Dy³⁺ doped TiO₂ powder calcined at a temperature of 300, 500 and 700 °C were shown in Figure 1. For TiO₂ the major peaks obtained at 2θ value at 25.18°, 37.94°, 48.07° and 54.15° were assigned to diffraction from the planes (101), (103), (200), (105), and (213) respectively. Dy³⁺ doped TiO₂ possess peaks at 2θ value at 25.52°, 38.00°, 48.20°, 54.52°, 62.80°, and 75.2° were corresponds to (101), (103), (200), (105), (213) and (107) planes respectively. These results are consistent with the data base of (JCPDS No 75-1537) of an anatase TiO₂. From the XRD pattern it is confirmed that both TiO₂ and Dy³⁺ doped TiO₂ are in anatase structure and Dy³⁺ doped TiO₂ calcined at 700°C shows more relative intensity of (101) peak than others. From Figure 1A, XRD patterns of Dy³⁺ doped TiO₂ at calcination temperature of 700°C shows a doublet at 2θ = 53.79 and 54.98° corresponding to the planes (105) and (211) where as in the TiO₂ sample this is turned to singlet peak at 2θ = 54.01° corresponding to (105) plane in the Dy³⁺ doped TiO₂ sample. From XRD spectra, it is clear that TiO₂ and Dy³⁺ doped TiO₂ showed complete anatase phase at all temperatures. Presence of complete anatase phase is due to the formation of Dy-O-Ti bond which inhibit the movement of Ti atoms for the phase transformation and that of bare TiO₂ may be due to the addition of acetic acid while synthesis, which stabilize the TiO₂ sol formed after hydrolysis. The relative intensity of (101) peaks increased significantly in Dy³⁺ doped TiO₂ with respect to the TiO₂. This confirms the Dy³⁺ doping induced higher crystallinity and phase purity in doped TiO₂.

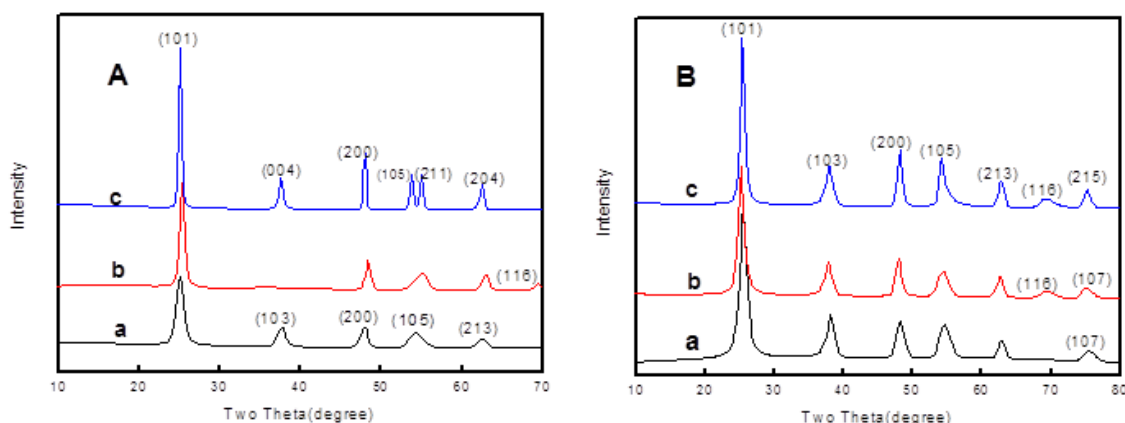


Figure.1.XRD pattern of A) TiO₂ B) Dy³⁺dopeTiO₂at a) 300 b) 500 and c) 700 °C

Crystalline size calculated for TiO₂ and Dy³⁺ doped TiO₂ using Sherr's equation were shown in Table 1. Crystallite sizes of TiO₂ calcined at temperature 300, 500 and 700 °C are 7.84, 12.6, and 21.7 nm respectively. Similarly crystallite size of Dy³⁺ doped TiO₂ calcined at 300, 500 and 700 °C was 7.2, 8.6 and 11.1 nm respectively. It is found that the crystallite size decreased by Dy³⁺ doping confirms the improvement in the nanocrystalline nature of TiO₂ as a result of Dy³⁺ doping. For TiO₂ crystallite size increases with calcination temperature. Dy³⁺ doped TiO₂ doped sample showed increase in crystallite size with all calcined temperature. From Table 1 it is clear that a drastic change in crystallite size occurs in the case of 700 °C calcined sample of TiO₂ to Dy³⁺ doped TiO₂. TiO₂ possess 21.7 nm, however Dy³⁺ doped TiO₂ possess only 11.1 nm. It indicates that upon doping crystallite size decreases and thus improves nano behavior of Dy³⁺ doped TiO₂. The decrease in crystalline size may attributed to the presence of Ti-O-Dy bond formation in the Dy³⁺ doped sample, which inhibits the growth of crystal grains.

Table 1. Crystallite size of TiO₂ and Dy³⁺ doped TiO₂ calcined at different temperatures

Sample	Crystallite size (nm)		
	300 °C	500 °C	700 °C
TiO ₂	7.84	12.6	21.7
Dy ³⁺ doped TiO ₂	7.2	8.6	11.1

3.2. FTIR Spectroscopy: The FTIR spectra of TiO₂ and Dy³⁺ doped TiO₂ calcined at 300 °C were shown in Figure 2. TiO₂ and Dy³⁺ doped TiO₂ sample possess strong and broad band in the range of 400-700 cm⁻¹ which were attributed to Ti-O stretching and Ti-O-Ti bridging stretching modes, which is a characteristic peaks of observable in the anatase phase of TiO₂. A new band at 405 cm⁻¹ was observed in the spectra of Dy³⁺ doped TiO₂ samples. This band is attributed to the Dy-O bond and it arises due to the reason that Dy³⁺ ions dispersed on the surface of TiO₂ in the form of metal oxides, formed during the calcination process. The peak at 1425, 1540 cm⁻¹ in both TiO₂ and Dy³⁺ doped TiO₂ is due to the symmetric and asymmetric stretching vibration of acetate groups. The band at 1625 cm⁻¹ and broad band at 3400 cm⁻¹ in both sample corresponding to the O-H bending and stretching modes of water indicative of the presence of residual water and hydroxyl groups present in the sample. Absorbed CO₂ on the surface is indicated by the peak on 2337 cm⁻¹. The peak at 2920 and 2855 cm⁻¹ is the asymmetric C-H stretching vibration. Absorbed CO₂ on the surface is indicated by the peak on 2337 cm⁻¹. The broad peak in the range 400-700 cm⁻¹ is due to Ti-O stretching vibration modes, which can be observable in the anatase phase of TiO₂. Band at 543 cm⁻¹ observed, attributes the Dy-O bond. Similar type of observation was also seen in the FTIR spectra of TiO₂ and Dy³⁺ doped TiO₂ calcined at 500 and 700 °C.

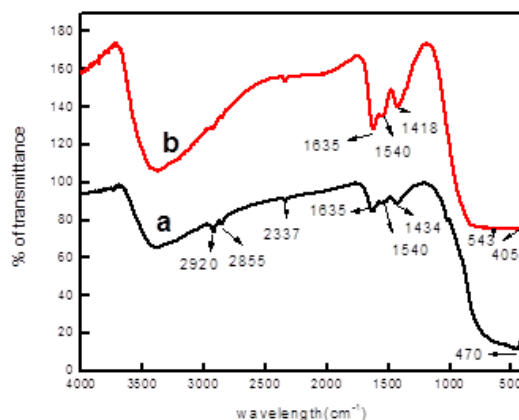


Figure 2. FTIR spectra of a) TiO₂ b) Dy³⁺ doped TiO₂ calcined at 300 °C

3.3. Optical Characterization: Diffuse Reflectance spectroscopy (DRS) was used to obtain the band gap energy value of TiO₂ and Dy³⁺ doped TiO₂ and were shown in Table 3. From DRS, it is clear that the bare TiO₂ has no absorption in the visible region (>400 nm), however the Dy³⁺-doped TiO₂ has showed significant absorption between 400 and 500 nm. Dy³⁺ doped TiO₂ sample (Figure 3) showed a significant shift to longer wavelengths and an extension of the absorption in to the visible region due to the doping effect of Dysprosium. Hence band gap energy of Dy³⁺ doped TiO₂ samples is lesser compared to TiO₂ at different calcinations temperature. Lin (1998), reported that the band gap of TiO₂ nanoparticles was reduced by Nd³⁺ doping and the band gap narrowing

was primarily attributed to the substitution Nd^{3+} ions which introduced electron states into the band gap of TiO_2 to form the new lowest unoccupied molecular orbital. Here FTIR already confirmed the presence of Dy^{3+} ion doped in the lattice of TiO_2 . The Dy^{3+} ion in TiO_2 lattice will introduce new electronic states into the band gap of TiO_2 to form the new lowest unoccupied molecular orbital that will expected to lead to the higher photocatalytic activity of Dy^{3+} doped TiO_2 .

Table 2. Band gap of TiO_2 and Dy^{3+} doped TiO_2 calcined at different temperatures.

Temperature ($^{\circ}\text{C}$)	Band gap(eV)	
	TiO_2	Dy^{3+} doped TiO_2
300	3.34	2.54
500	3.32	2.51
700	3.05	2.49

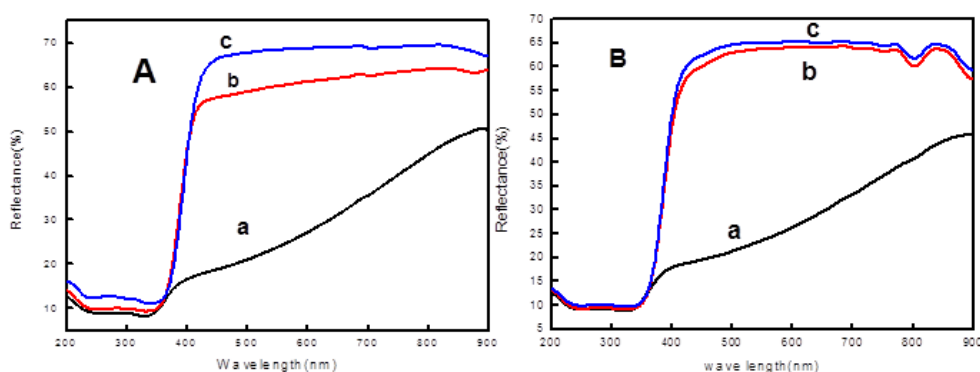


Figure.3. Diffuse Reflectance Spectra of A) TiO_2 B) Dy^{3+} doped TiO_2 at a) 300 b) 500 c) 700 $^{\circ}\text{C}$

3.4. Transmission Electron Microscope (TEM): TEM images of TiO_2 and Dy^{3+} doped TiO_2 calcined at 700 $^{\circ}\text{C}$ were shown in Figure 4. TiO_2 shows a crystallite size of 18–28nm (Fig. 4a) at 700 $^{\circ}\text{C}$. On the other hand, the Dy^{3+} doped TiO_2 has a crystallite size of 7-14nm (Fig. 4b), and thus the TEM observations support the conclusions derived from the XRD data. The electron diffraction image of Dy^{3+} doped TiO_2 calcined at 700 $^{\circ}\text{C}$ shows broad bands due to the Scherrerline broadening which is attributed to the small crystallite size however TiO_2 , at same temperature, showed distinct spots due to the high crystallinity and larger size of the crystals.

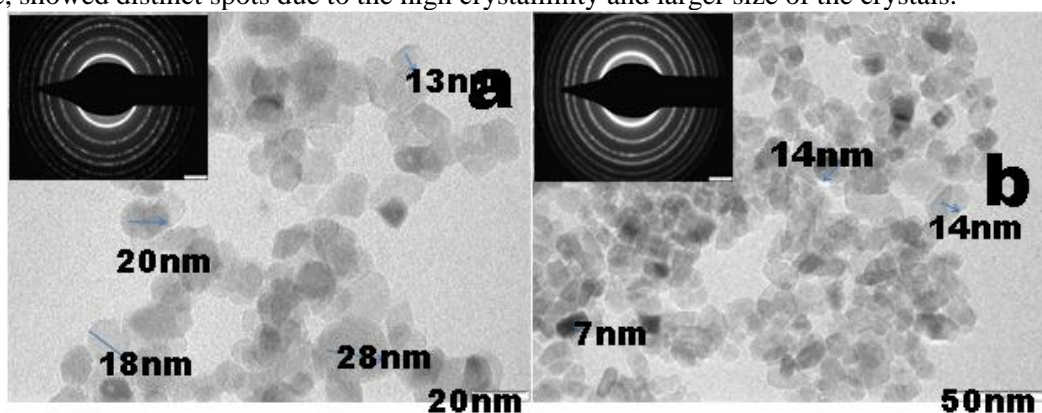


Figure.4. TEM image of a) TiO_2 b) Dy^{3+} doped TiO_2 at 700 $^{\circ}\text{C}$

3.5. Photocatalytic activity of TiO_2 and Dy^{3+} doped TiO_2 : Under irradiation from a suitable light source applied to the TiO_2 material, the electrons in the TiO_2 valence band will be excited, causing the electron to jump to the conduction band resulting in formation of a positive hole in the valence band and a free electron in the conduction band. These photogenerated electrons are able to reduce the dioxygen molecule to produce superoxide radicals and the hole can simultaneously oxidize water to produce hydroxyl radicals. These radicals are highly reactive and are able to break chemical bonds. This makes TiO_2 , a suitable photocatalyst useful in the field of environmental

purification. Textile dyes and other industrial dye stuffs constitute one of the largest groups of organic compounds that represent an increasing environmental danger. Methylene Blue is a kind of typical azo dye used in the textile dye industry. Here we selected methylene blue dye as a target of photodegradation due to these practical values. The photocatalytic activity of the samples is executed by the degradation using aqueous solution of methylene blue. Before irradiating with a UV lamp light, the samples were stirred in the dark for fifteen minutes. Results of absorption spectra showed that the methylene blue concentration has negligible decrease caused by the slight absorption on photocatalysts surface, which indicates that there is no degradation in the absence of irradiation. When photocatalytic reaction is conducted in aqueous medium, the holes were effectively scavenged by the water and generated hydroxyl radicals $\text{OH}\cdot$, which are strong and unselected oxidant species in respect of total oxidative degradation for organic substrates. The holes, free electron, superoxide and hydroxyl radicals have been proposed as the oxidizing and reducing species responsible for the degradation (mineralization) of the organic substrates.

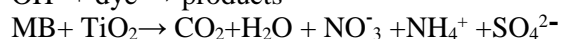
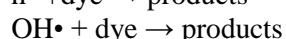
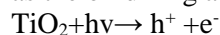


Table.3. Degradation time and rate constant in min under UV light of samples at different calcination temperatures

Temperature (°C)	TiO ₂		Dy ³⁺ doped TiO ₂	
	Time (min)	Rate constant	Time (min)	Rate constant
300	150	0.021	105	0.007
500	70	0.037	40	0.051
700	210	0.003	60	0.070

Photocatalytic activity of both TiO₂ and Dy³⁺ doped TiO₂ for methylene blue degradation under UV light are summarized in the Table 3. From the Table 3, it is observed that at Dy³⁺ doped TiO₂ sample showed greater photocatalytic activity than TiO₂ under UV light. The rate constant calculated from the first order kinetics were also shown in the Table 3. Among the Dy³⁺ doped TiO₂ maximum activity was obtained for sample calcined at 700 °C. The highest rate constant 0.070 min⁻¹ corresponds to the Dy³⁺ doped TiO₂ at 700°C while its TiO₂ counterpart has only 0.003 min⁻¹. Absorption spectra of methylene blue dye degradation under UV using TiO₂ and Dy³⁺ doped TiO₂ at 700 °C were shown in Figure 6. Therefore it can be concluded that the Dy³⁺ doped TiO₂ calcined at 700 °C is the best photocatalyst among these samples under UV light irradiation, showing the fastest decolourization of methylene blue and has the maximum degradation rate constant.

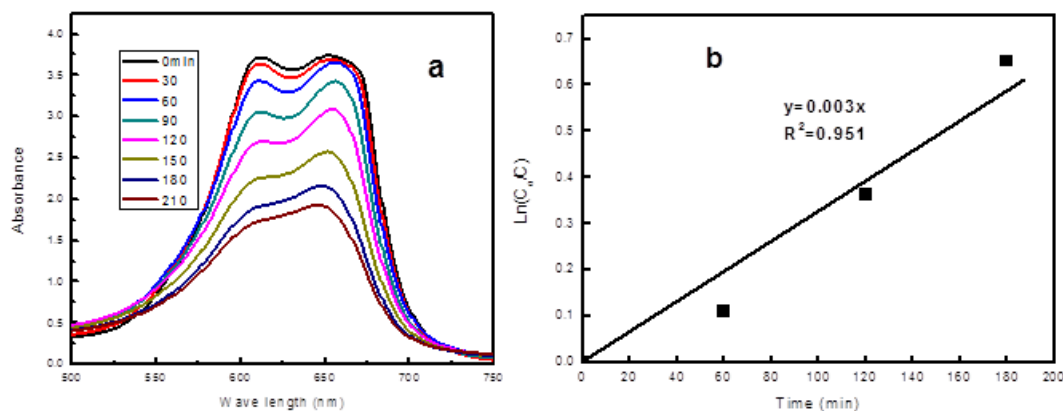


Figure.5. Absorption spectra and Kinetic study of methylene blue dye degradation under UV using TiO₂ sample calcined at 700°C, C₀ is the Initial absorbance and C is the absorbance after a time of the methylene blue dye degradation

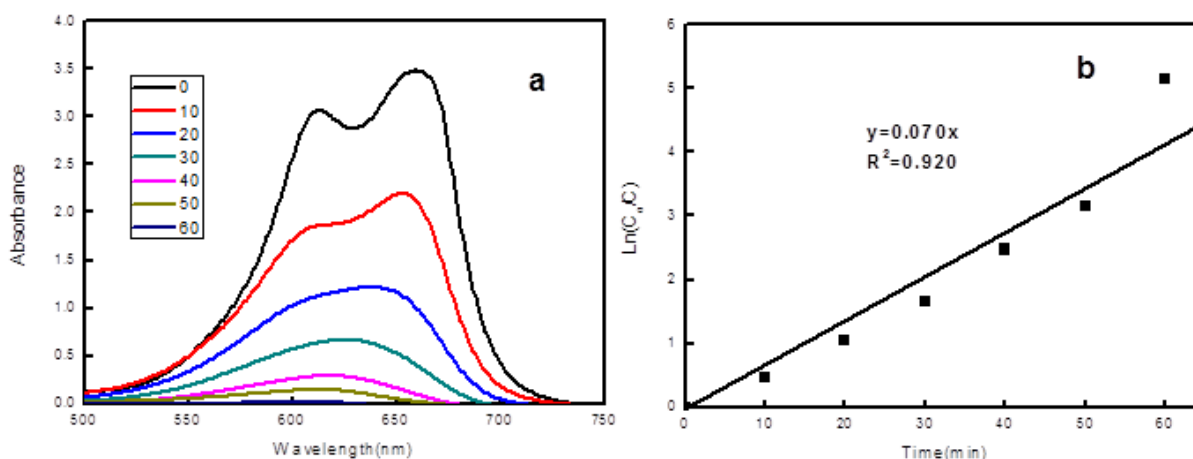


Figure.6. Absorption spectra and Kinetic study of methylene blue dye degradation under UV using Dy^{3+} doped TiO_2 sample calcined at $700^\circ C$, C_0 is the Initial absorbance and C is the absorbance after a time of the methylene blue dye degradation

4. CONCLUSIONS

Nanocrystalline TiO_2 and Dy^{3+} doped TiO_2 has been successfully synthesized using a modified sol-gel method. The samples were calcined at 300, 500 and $700^\circ C$ and characterized by various techniques such as XRD, UV/Vis Reflectance spectroscopy, FTIR and TEM. XRD study proved that both TiO_2 and Dy^{3+} doped TiO_2 sample synthesised are in the form of anatase phase. TEM study confirmed that TiO_2 has a crystallite size of 18–28 nm, on the other hand, the Dy^{3+} doped TiO_2 has a size of 7–14 nm, revealed that the doping Dy^{3+} ion decreased the crystallite size of TiO_2 and thereby induced more nano behavior. FTIR spectroscopy confirmed Ti-O and Ti-O-Ti bond in TiO_2 , in Dy^{3+} doped TiO_2 presence of Dy-O and Ti-O-Dy bonds are also been confirmed along with Ti-O and Ti-O-Ti bond. Diffuse reflectance spectra showed that the Dy^{3+} doped TiO_2 have a significant red shift and an extension of the absorption in the visible region compared to the TiO_2 . Finally the photocatalytic activity of TiO_2 and Dy^{3+} doped TiO_2 at various calcination temperatures was investigated by the degradation of methylene blue solution under UV light. Doping with the Dy^{3+} significantly enhanced the overall photocatalytic activity for MB degradation under UV light irradiations. The results showed that the Dy^{3+} doped TiO_2 sample calcined at $700^\circ C$ shows the highest photocatalytic activity under UV light irradiation. These high temperature stable and higher photoactive Dy^{3+} doped anatase TiO_2 may be used for the self-cleaning, white light emitting and antibacterial coatings on high temperature processed ceramic materials.

REFERENCES

- Arslan-Aloton, Advanced oxidation of textile industry dyes, S. Parsons (Ed.), IWA Publishing, London, 2004, 302–308.
- Ayca Kambur, Guln Selda Pozan, Ismail Boz, Preparation, characterization and photocatalytic activity of TiO_2 – ZrO_2 binary oxide nanoparticles, Appl. Catal. B: Environ., 115, 2012, 149–158.
- Baiju K.V, Siblu C.P, Rajesha K, Pillai P.K, Mukundan P, Warriar K.G.K, Wunderlich W, An aqueous sol–gel route to synthesize nanosized lanthana-doped titania having an increased anatase phase stability for photocatalytic application, Mater. Chem. Phys., 90, 2005, 123–127.
- Borgarello E, Kiwi J, Gratzel M, Pelizzetti E, Visca M, Visible light induced water cleavage in colloidal solutions of chromium-doped titanium dioxide particles, J. Am. Chem. Soc., 104, 1982, 2996–3002.
- Chockalingam Karunakaran, Binu Naufal, and Paramasivan Gomathisankar, Efficient Photocatalytic Degradation of Salicylic Acid by Bactericidal ZnO. J.Kor.Chem.Soc., 56, 2012, 108–114.

Houas A, Lachheb H, Ksibi M, Elalooui E, Guillard C, Herrmann J.M, Photocatalytic degradation pathway of methylene blue in water, *App. Catal. B Environ.*, 31, 2001, 145–157.

Karkmaz M, Puzenat E, Guillard C, Herrmann J.M, Photocatalytic degradation of the alimentary azo dye amaranth - Mineralization of the azo group to nitrogen, *App.Catal. B Environ.*, 51, 2004, 183–194.

Lin J, Yu J.C, An investigation on photocatalytic activities of mixed TiO₂-rare earth oxides for the oxidation of acetone in air, *J. Photochem. Photobiol. Chem.A*, 116, 1998, 63-67.

Parida K.M, Sahu N, Visible light induced photocatalytic activity of rare earth titania nanocomposites, *J. Mol. Catal. A: Chem.*, 287, 2008, 151-158.

Periyat P, McCormack D.E, Colreavy J, Hinder S.J, Pillai S.C, Improved High-Temperature Stability and Sun-Light-Driven Photocatalytic Activity of Sulfur-Doped Anatase TiO₂, *J. Phys. Chem. C*, 112, 2008, 7644-7652.

Periyat P, McCormack D.E, Hinder S.J, Pillai S.C, One-Pot Synthesis of Anionic (Nitrogen) and Cationic (Sulfur) Codoped High-Temperature Stable, Visible Light Active, Anatase Photocatalysts, *J.Phys.Chem.C*, 113, 2009, 3246-3253.

Periyat P, Saeed P.A, Ullattil S.G, Anatase titania nanorods by pseudo-inorganic templating. *Mater. Sci. Semicond. Process.*, 31, 2015, 658-664.

Sudha M, Senthilkumar S, Hariharan R, Suganthi A, Rajarajan M, Synthesis, characterization and study of photocatalytic activity of surface modified ZnO nanoparticles by PEG capping, *J.Sol-Gel Sci.Technol.*, 65, 2013, 301–310.

Tayade R.J, Bajaj H.C, Jasra R.V, Transition Metal Ion Impregnated Mesoporous TiO₂ for Photocatalytic Degradation of Organic Contaminants in Water, *Ind. Eng. Chem. Res.*, 45, 2006, 5231-5238.

Xiao Q, Si Z, Zhang J, Xiao C, Tan X, Photo induced hydroxyl radical and photocatalytic activity of samarium-doped TiO₂ nanocrystalline, *J. Hazard. Mater.*, 150, 2008, 62-67.